

# Guided wave analysis of air-coupled impact-echo in concrete slab

Hajin Choi\* and Hoda Azari

Federal Highway Administration, 6300 Georgetown Pike, McLean, Virginia, 22101, USA

(Received July 24, 2017, Revised August 14, 2017, Accepted August 17, 2017)

**Abstract.** This study aims to develop a signal processing scheme to accurately predict the thickness of concrete slab using air-coupled impact-echo. Air-coupled impact-echo has been applied to concrete non-destructive tests (NDT); however, it is often difficult to obtain thickness mode frequency due to noise components. Furthermore, apparent velocity in concrete is a usually unknown parameter in the field and the thickness of the concrete slab often cannot be accurately measured. This study proposes a signal processing scheme using guided wave analysis, wherein dispersion curves are drawn in both frequency-wave number ( $f$ - $k$ ) and phase velocity-frequency ( $V_{cp}$ - $f$ ) domains. The theoretical and experimental results demonstrate that thickness mode frequency and apparent velocity in concrete are clearly obtained from the  $f$ - $k$  and  $V_{cp}$ - $f$  domains, respectively. The proposed method has great potential with regard to the application of air-coupled impact-echo in the field.

**Keywords:** concrete; concrete technology; non-destructive tests (NDT); structural health monitoring (SHM); structural safety

## 1. Introduction

In non-destructive tests (NDTs) in civil engineering, computations such as signal processing are necessary to improve the quality of measurements or to analyze raw data (Wright 2010, Munoz-Abella *et al.* 2012, Sadeghi and Rezvani 2013, Gholizadeh *et al.* 2015, Ji *et al.* 2015, Chatzi *et al.* 2015). Mechanical wave methods in concrete NDTs provide a direct relation to the elastic properties of inspected concrete; however, the measurements are sometimes limited due to the heterogeneity of the concrete to high damping ratio (Alexandridis *et al.* 2015, Kibar and Öztürk 2015, Hung *et al.* 2017). Furthermore, the obtained waveforms are usually affected by noise components from the environment or the data acquisition system. To overcome the limitations and to improve the low signal to noise ratio, signal processing has been investigated as an important procedure in concrete NDTs (Sheena *et al.* 2013, Ongpeng *et al.* 2017, Kim *et al.* 2017).

In concrete NDTs, impact-echo has been applied to concrete slab or pavement to estimate their thickness (Carino *et al.* 1986). Using a simple test set-up including one impactor and one sensor, propagating waves are recorded and analyzed in the frequency domain. However, contact-based sensing technology is significantly limited with regard to measurement because of the rough surface of concrete and the high acoustic impedance mismatch a between Piezo-electrical type sensor and concrete. Air-coupled sensing possibly overcomes the practical problem related to measurement. Without a physical coupling process, air-coupled sensing measures a leaky portion of

waves, which have the same characteristics as the propagating waves in concrete.

Although air-coupled impact-echo has been introduced in the civil engineering domain (Zhu and Popovics 2007), no practical application of it to thickness measurements has been reported. This is mainly because of the weak energy portion of the leaky waves in the air. Many researchers have investigated the secondary efforts on thickness mode frequency detection using air-coupled impact-echo; Zhu and Popovics (2007) suggest acoustic isolation around the microphone and Dai *et al.* (2011) apply parabolic reflectors to amplify signals. Furthermore, Bjurström and Ryden (2016) propose the concept of backward wave propagation using dispersion relations. In terms of hardware improvement, microelectromechanical systems (MEMS) have recently been introduced and applied to air-coupled sensing technology and concrete NDTs (Groschup and Grosse 2015, Choi *et al.* 2016). The small size and high sensitivity have great potential to develop air-coupled sensing systems. Therefore, an effective post-processing algorithm using the measurements from air-coupled sensing has been required.

This paper describes the procedure of developing a signal processing scheme based on guided wave analysis in order to improve the measurement of the thickness of concrete slab using air-coupled sensing technology. Two different approaches using the same signal data are applied; frequency-wave number domain analysis using two-dimensional Fourier transform, and phase velocity-frequency domain analysis using selective offset scheme. Each method generates experimental dispersion relations and provides the thickness mode frequency and surface wave velocity, respectively. The main contribution of this paper is the suggestion of a signal processing scheme to improve the procedure used to estimate thickness using air-coupled impact-echo. Notably, the proposed method could

---

\*Corresponding author, Ph.D.  
E-mail: [dr.hajin.choi@gmail.com](mailto:dr.hajin.choi@gmail.com)

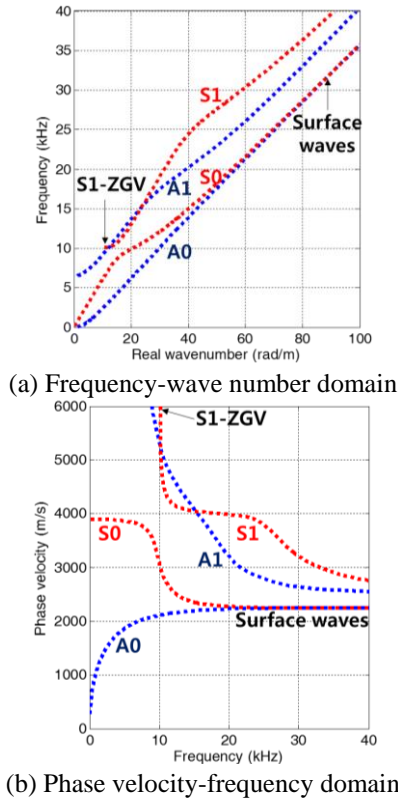


Fig. 1 Theoretical dispersion curves of a 190.5-mm concrete plate with a Poisson's ratio of 0.2

possibly enable the detection of impact-echo frequency among noise components and the experimental measurement of surface wave velocity, which cannot be obtained using a conventional impact-echo analysis. The theoretical dispersion curves and experimental examples demonstrate the effectiveness of the proposed signal processing scheme with regard to the application of air-coupled impact-echo.

## 2. Guided wave analysis

In this study, a signal processing scheme using a guided wave analysis is proposed to detect impact-echo frequency and to identify apparent velocity in concrete with regard to the application of the air-coupled sensing technology. The impact-echo method has been used to estimate the thickness ( $D$ ) of concrete slab or delamination using the following formula

$$D = \frac{\beta V_p}{2f_{IE}} \quad (1)$$

where  $V_p$  is the P-wave velocity of the concrete,  $f_{IE}$  is the thickness mode frequency measured using a test, and  $\beta$  is the correction factor (0.96) for apparent velocity ( $\beta V_p$ ) in concrete (ASTM 2015). Because it is difficult to accurately measure apparent velocity in concrete using the test, thickness estimates obtained using Eq. (1) are usually erroneous. Although the ASTM standard suggests measuring P-wave velocity using two sensors in a row, the

measurement is limited due to the significantly small amplitude of P-waves.

Air-coupled sensing technology has been applied to concrete NDTs; however, data acquisition is affected by environmental noise and important information is sometimes misled. In the case of an impact-echo test, the thickness mode frequency is significantly affected by direct acoustic noise from the impactor, unlike the flexural mode (Zhu and Popovics 2007, Oh *et al.* 2013, Kee and Gucunski 2016). Therefore, it is difficult to obtain the thickness mode frequency using a conventional impact-echo analysis such as one-dimensional Fourier transform. The proposed guided wave analysis enables the detection of the thickness mode frequency among the noise and different wave components as described in the following sections.

### 2.1 Dispersion relation

After the impact source is applied to the surface of concrete, waves start to propagate and are guided by the geometrical boundary condition of the structure. In the case of plate-like structures such as slab and pavement, the plate exhibits two different vibration behaviors; symmetric (S) and anti-symmetric (A) modes. The symmetric mode of the vibration behaviors is defined by a Lamb-Rayleigh frequency equation

$$\frac{\tan qh}{\tan ph} = -\frac{4k^2pq}{(q^2 - k^2)^2} \quad (2)$$

with  $p$  and  $q$  given as

$$p = \sqrt{\frac{\omega^2}{c_p^2} - k^2}, \quad q = \sqrt{\frac{\omega^2}{c_s^2} - k^2} \quad (3)$$

where  $h$  is the thickness of the plate,  $k$  is the wave number,  $\omega$  is the angular frequency, and  $c_p$  and  $c_s$  are the P- and S-wave velocity, respectively. In dispersive media, each frequency component of waves has a different phase velocity and wave number. In the plate-like structures, the dispersion relation is defined as dispersion curves, which are obtained using a numerical solution, Eq. (2). As shown in Fig. 1, theoretical dispersion curve is drawn in frequency-wave number ( $f$ - $k$ ) domain and phase velocity-frequency ( $V_{cp}$ - $f$ ) domain, respectively. The material properties used in the dispersion curves are presented in Table 1. The first two modes from each S and A vibration are plotted.

The thickness mode frequency in impact-echo test has been discovered that the frequency is same as the frequency at zero-group velocity motion of the first symmetric mode (S1-ZGV) from the guided waves in plate (Gibson and Popovics 2005). Because the S1-ZGV has zero velocity, the waves are not propagating in the plate, and the plate vibrates at resonance frequency. This specific motion has been investigated and demonstrated in the field of non-destructive evaluation and material characterization (Clorennec *et al.* 2007, Prada and Clorennec 2009, Gomez *et al.* 2017). From the example of the concrete slab case shown in Fig. 1(a), the S1-ZGV is formed at a frequency of around 10 kHz and a wave number of around 10 rad/m. The

Table 1 Summary of material properties in theoretical dispersion curves

Thickness (mm)	Young's modulus (MPa)	Poisson's ratio	Density (kg/m <sup>3</sup> )	P-wave velocity (m/s)	S-wave velocity (m/s)
190.5	35	0.2	2400	4025	2465

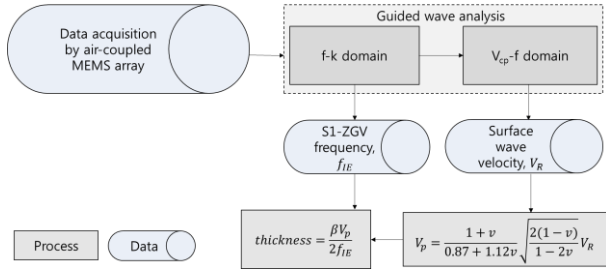


Fig. 2 The proposed signal processing scheme

vibration motion of the S1-ZGV consists of P- and S- wave velocity as shown in Eq. (3) so that a correction factor is needed in Eq. (1) where only P-wave velocity is considered.

While the frequency-wave number domain clearly shows the S1-ZGV as the zero-slope of the S1 curve, the phase velocity-frequency domain is limited to representing the S1-ZGV. The phase velocity-frequency domain better represents surface waves in the high frequency region (above 20 kHz in this example). The A0 and S0 modes are combined in high frequency and the velocity of the waves becomes identical to the surface wave velocity. The phase velocity-frequency domain analysis has been used in the form of a multichannel analysis of surface waves (MASW) (Park 2011, Bjurstrom and Ryden 2016). In MASW, the impact source moves with regular spacing while one sensor is fixed. Although the measurement procedure in MASW is reciprocal of the applied hardware presented in this study (multiple sensing and a fixed source), the analysis scheme is equivalent. Using the dispersion characteristics of the waves in concrete slab, the thickness mode frequency and surface wave velocity can be experimentally measured, and the obtained values can be plugged into Eq. (1) for thickness estimation.

## 2.2 Signal processing

The procedure of the proposed analysis scheme is illustrated in Fig. 2. After measuring the waveforms using an air-coupled MEMS array, experimental dispersion relations are generated using two-dimensional Fourier transform for the frequency-wave number domain and the selective offset scheme for the phase velocity-frequency domain (Song and Popovics 2017, Choi *et al.* 2017, Park 2011). Both signal processing methods represent the energy portion of the wave modes; however, the represented energy has different physical meaning; the f-k domain shows the magnitude of the Fourier transform product while the  $V_{cp}$ -f domain represents the amplitude of the phase velocity per digitized frequency. Using guided wave analysis in each domain, thickness mode frequency and apparent velocity in concrete can be obtained, respectively.

In the phase velocity-frequency domain, surface wave velocity ( $V_R$ ) can be used to estimate P-wave velocity ( $V_p$ )

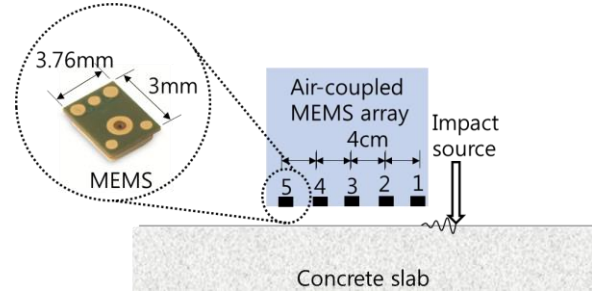


Fig. 3 Schematic illustration of air-coupled impact-echo and MEMS array

using the following equation

$$V_p = \frac{1 + \nu}{0.87 + 1.12\nu} \sqrt{\frac{2(1 - \nu)}{1 - 2\nu}} V_R \quad (4)$$

where  $\nu$  is Poisson's ratio (Popovics *et al.* 1998). With the assumption of concrete Poisson's ratio (0.2 in general concrete), P-wave velocity is also estimated. The correction factor is also a function of Poisson's ratio (Gibson and Popovics 2005)

$$\beta = -0.645\nu^2 + 0.135\nu + 0.952 \quad (5)$$

Using Eq. (5), the correction factor in concrete varies from 0.945 to 0.957 in concrete. With the correction factor and P-wave velocity, the apparent velocity in concrete can be obtained.

In the frequency-wave number domain, the thickness mode frequency is easily obtained at the frequency of S1-ZGV mode, where the S1 curve has zero slope. Because the phase velocity of the mode is much faster than the direct acoustic noise (the velocity in air), the S1-ZGV mode is clearly detected in frequency-wave number domain.

Using the obtained thickness mode frequency from S1-ZGV and apparent velocity from surface wave velocity, the thickness of inspected concrete slab can be estimated based on Eq. (1) with minimal error. Note that all computations in the signal processing procedure are performed using Matlab platform. Because all computations are performed using built-in functions such as fast Fourier transform, the total processing duration is less than 3 seconds using a personal computer.

## 3. Air-coupled sensing technology

### 3.1 Air-coupled MEMS array

The air-coupled MEMS array was developed for the application of air-coupled impact-echo in the field. The array consists of twenty units of MEMS (Knowles SPU0410LR5H-QB) with a designed amplifying circuit board. Each MEMS has the following dimensions: a width of 3.76 mm, a length of 3 mm, and a thickness of 1.1 mm. Nominal sensitivity is 94 dB at 1kHz. The MEMS are spatially placed onto the board at regular 1-cm spacing. Note that only five MEMS with 4-cm spacing are used in this study. The MEMS has great potential for concrete NDTs due to its small dimension and high sensitivity by 50

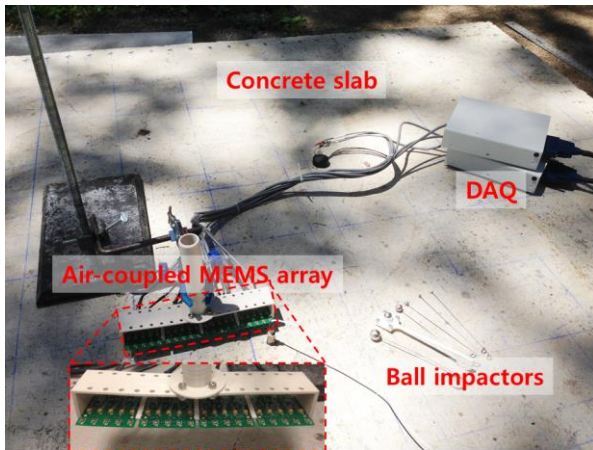


Fig. 4 Test set-up

kHz. The small spacing between sensors is important in the array system and guided wave analysis as it serves to reduce spatial aliasing issues in practical measurement. Note that an acoustic barrier is placed between the air-coupled MEMS array and the impactor to minimizing spatial aliasing in this study.

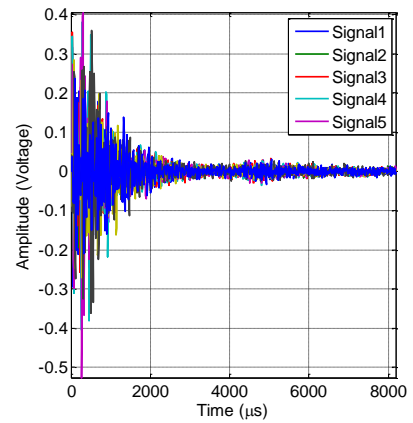
### 3.2 Test set-up

Air-coupled impact-echo tests were performed with concrete slab. The experimental set-up is presented in Fig. 4. The size of the concrete slab is 2 m by 2 m while the thickness is 190.5 mm. Concrete is composed of aggregate with a maximum size of 20 mm, and the slab does not contain reinforcement. The signals are digitized at 125 kS/s using NI PXI 6255. The air-coupled MEMS array is placed at the center of the slab with a 2-cm air-gap. The air-gap can be larger than 2 cm in practical terms; however, there is a greater chance of measuring environmental noise in a larger air-gap distance. Conventional steel ball impactors are applied to this test.

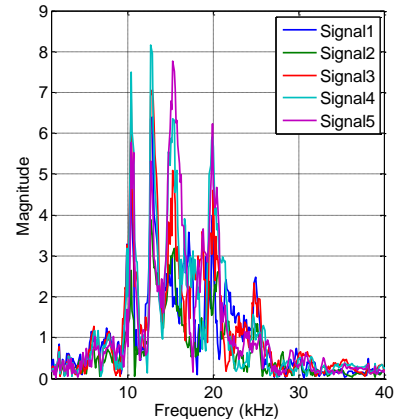
## 4. Experimental results

### 4.1 Conventional impact-echo analysis

The signal data obtained using the air-coupled MEMS array is processed based on conventional impact-echo analysis. The results are plotted in Fig. 5, including the signals in the time and frequency domains. One-dimensional time Fourier transform was applied to the signal data. As shown in Fig. 5(b), four frequency components are significantly dominant and the thickness mode frequency is not clearly identified among them. This is because the air-coupled MEMS array measures all wave modes including the thickness mode, surface waves and noise components. The noise is mainly from direct waves caused by the applied impactor. The frequency component of direct waves usually disturbs the detection of the thickness mode in the frequency domain because of similar frequency profiles. An additional signal processing scheme is required in air-coupled impact-echo to identify the



(a) Signals in time domain



(b) Signals in frequency domain

Fig. 5 Conventional impact-echo analysis using one-dimensional Fourier transform

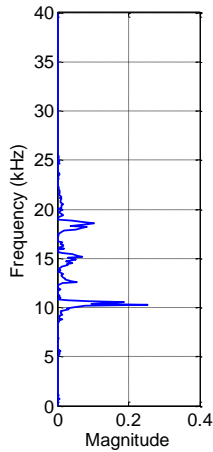
thickness mode frequency among the other frequency components.

### 4.2 Frequency-wave number domain

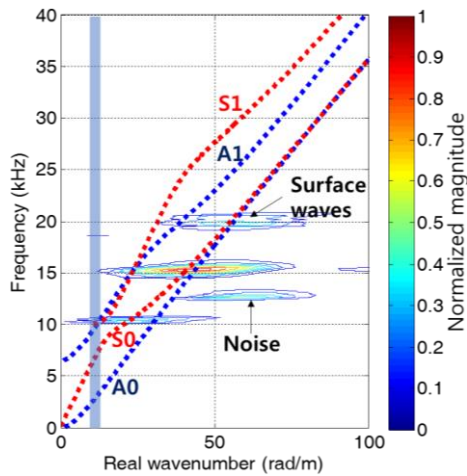
In the frequency-wave number domain, the specific wave number at S1-ZGV can be extracted to detect the thickness mode frequency (Choi *et al.* 2017). The two-dimensional Fourier transform is applied to the signal data in time and space. Note that the Nyquist wave number is 78.5 rad/m while the spectral line spacing of wave number is 0.15 rad/m after zero padding. The magnitude of the transform product is plotted as a jet color scheme, and theoretical dispersion curves developed from Fig. 1 are drawn in the same domain. Experimental dispersion relations present relative energy portions in frequency as well as in wave number. Unlike the one-dimensional time Fourier transform shown in Fig. 5(b), the thickness mode frequency at S1-ZGV is distinguished from the other wave modes and noise components. Note that direct noise from the impactor is around 12 kHz and the energy portion is not placed onto theoretical dispersion curves because the noise is not guided waves.

### 4.3 Phase velocity-frequency domain

In the frequency-wave number domain, the specific



(a) Frequency components at wave number 10 rad/m



(b) Frequency-wave number domain (blue shaded box represents the frequency components at wave number 10 rad/m)

Fig. 6 Frequency-wave number domain analysis

wave number at S1-ZGV can be extracted to detect the thickness mode frequency (Choi *et al.* 2017). The two-dimensional Fourier transform is applied to the signal data in time and space. Note that the Nyquist wave number is 78.5 rad/m while the spectral line spacing of wave number is 0.15 rad/m after zero padding. The magnitude of the transform product is plotted as a jet color scheme, and theoretical dispersion curves developed from Fig. 1 are drawn in the same domain. Experimental dispersion relations present relative energy portions in frequency as well as in wave number. Unlike the one-dimensional time Fourier transform shown in Fig. 5(b), the thickness mode frequency at S1-ZGV is distinguished from the other wave modes and noise components. Note that direct noise from the impactor is around 12 kHz and the energy portion is not placed onto theoretical dispersion curves because the noise is not guided waves.

Similar to the frequency-wave number domain, the dispersion relations are plotted in the phase velocity-frequency domain as shown in Fig. 7. Although the experimental dispersion relations are noisy, the amplitude of the phase velocity represented using a black color in Fig. 7 is clearly converged in high frequency, where S0 and A0

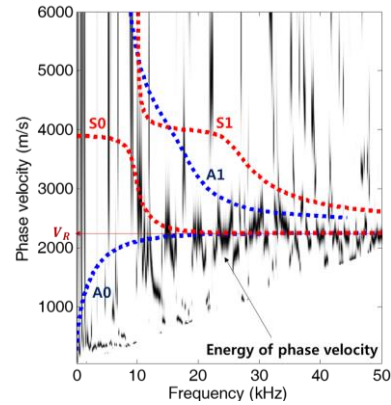


Fig. 7 Phase velocity-frequency domain analysis (black color represents the energy of phase velocity)

modes are combined. The selective offset scheme first allocates the spectral line spacing of frequency and iteratively calculates the energy of the phase velocity using the Fourier transform product. Because different wave modes are simultaneously calculated at each frequency step, the relative energy (black color) is not focused on one phase velocity and the black lines are a blur. The corresponding surface wave velocity is 2244 m/s and the P-wave velocity is calculated as 4020 m/s using Eq. (4). The Poisson's ratio is assumed to be 0.2 and the correction factor ( $\beta$ ) and apparent velocity in concrete are 0.953 and 3831 m/s, respectively.

With the thickness mode frequency and apparent velocity in concrete obtained using the guided wave analysis, the thickness of the concrete slab is estimated using Eq. (1) as 186.7 mm, where Poisson's ratio is assumed as 0.2. The error is less than 4 mm, which is acceptable in the field of civil engineering. Note that a Poisson's ratio of 0.22 gives the best result in this example with an error of less than 1 mm. The assumed Poisson's ratio affects the test result; however, the error is within the acceptable range in civil engineering, and Poisson's ratio in general concrete case has a small range of variation.

Several discussions can be drawn in this study. First, in terms of the thickness mode frequency detection, the comparison between Fig. 5(b) and Fig. 6(a) clearly show the effectiveness of the frequency-wave number domain analysis over the conventional ways. However, the S1-ZGV has a non-zero wave number, which is a function of the thickness of inspected structures and Poisson's ratio. Although Poisson's ratio does not vary significantly in concrete, the thickness information is needed to estimate the wave number at S1-ZGV. Second, only five MEMS are used in this study, which is a limited number of sensors for a guided wave analysis. It is difficult to generate an experimental dispersion relation with a smaller number of sensors. Third, smaller spacing between sensors is critical to minimize spatial aliasing. Also, an acoustic barrier is necessary to avoid the interference of direct waves. Because the direct waves have a velocity of 343 m/s and large wave numbers, the components can be spatially aliased in the f-k domain. To avoid this potential problem, we are currently improving the air-coupled MEMS array using more sensors

with narrower spacing.

## 5. Conclusions

This study proposed a signal processing procedure to predict the thickness of concrete slab using air-coupled impact-echo. The results from theoretical dispersion curves and experimental dispersion relations demonstrate that the guided wave analysis improves accuracy of thickness estimations of concrete slab made using air-coupled impact-echo.

- The conventional impact-echo analysis is limited in its ability to detect the thickness mode frequency because of noise components measured by air-coupled sensing.
- The thickness mode frequency is accurately obtained as same as the zero-group velocity of the first symmetric mode in the frequency-wave number domain.
- The apparent velocity is estimated based on an assumed Poisson's ratio and the measurement of surface wave velocity in the phase velocity-frequency domain.
- Using the proposed signal processing scheme, the thickness estimation of the concrete slab is 186.7 mm, which has an error of 3.8 mm.

## Acknowledgments

The work reported here was made possible with the support of the National Research Council Research Associateship Programs. The authors are grateful for the important contributions to the experimental hardware made by Infratek Solutions, Inc.

## References

- ASTM C1383-15 (2015), *Standard Test Method for Measuring the P-Wave Speed and the Thickness of Concrete Plates Using the Impact-Echo Method*, ASTM International, West Conshohocken, Pennsylvania, U.S.A.
- Bjurstrom, H. and Ryden, N. (2016), "Detecting the thickness mode frequency in a concrete plate using backward wave propagation", *J. Acoust. Soc. Am.*, **139**(2), 649-657.
- Carino, N.J., Sansalone, M. and Hsu, N.N. (1986), "A point source-point receiver, pulse-echo technique for flaw detection in concrete", *ACI J.*, **83**(2), 199-208.
- Chatzi, E.N. and Fuggini, C. (2015), "Online correction of drift in structural identification using artificial white noise observations and an unscented Kalman filter", *Smart Struct. Syst.*, **16**(2), 295-328.
- Choi, H., Shams, S. and Azari, H. (2017) "Frequency-wave number domain analysis of air-coupled impact-echo in concrete slab", *J. Infrastr. Syst.*
- Choi, H., Song, H., Tran, Q.N., Roesler, J.R. and Popovics, J.S. (2016), "Contactless system for continuous monitoring of early-age concrete properties", *Concrete Int.*, **38**(9), 35-41.
- Clorennec, D., Prada, C. and Royer, D. (2007), "Local and noncontact measurements of bulk acoustic wave velocities in thin isotropic plates and shells using zero group velocity Lamb modes", *J. Appl. Phys.*, **101**, 034908.
- Dai, X., Zhu, J., Tsai, Y.T. and Haberman, M.R. (2011), "Use of parabolic reflector to amplify in-air signals generated during impact-echo testing", *J. Acoust. Soc. Am.*, **130**(4), EL167-EL172.
- Gholizadeh, S., Leman, Z. and Baharudin, B.T.H.T. (2015), "A review of the application of acoustic emission technique in engineering", *Struct. Eng. Mech.*, **54**(6), 1075-1095.
- Gibson, A. and Popovics, J.S. (2015), "Lamb wave basis for impact-echo method analysis", *J. Eng. Mech.*, **131**(4), 438-443.
- Gomez, P., Fernandez-Alvarez, J.P., Ares, A. and Fernandez, E. (2017), "Guided-wave approach for Spectral peaks characterization of impact-echo tests in layered systems", *J. Infrastr. Syst.*, **1**(1), 0417009.
- Groschup, R. and Grosse, C.U. (2015), "MEMS microphone array sensor for air-coupled impact-echo", *Sensor.*, **15**(7), 14932-14945.
- Hung, C.C., Lin, W.T., Cheng, A. and Pai, K.C. (2017), "Concrete compressive strength identification by impact-echo method", *Comput. Concrete*, **20**(1), 49-55.
- Ji, Q., Ho, M., Zheng, R., Ding, Z. and Song, G. (2015), "An exploratory study of stress wave communication in concrete structures", *Smart Struct. Syst.*, **15**(1), 135-150.
- Kee, S.H. and Gucunski, N. (2016), "Interpretation of flexural vibration modes from impact-echo testing", *J. Infrastr. Syst.*, **22**(3), 04160009.
- Kibar, H. and Öztürk, T. (2015), "Determination of concrete quality with destructive and non-destructive methods", *Comput. Concrete*, **15**(3), 473-484.
- Kim, G.J., Park, S.J. and Kwak, H.G. (2017), "Experimental characterization of ultrasonic nonlinearity in concrete under cyclic change of prestressing force", *Comput. Concrete*, **19**(5), 599-607.
- Munoz-Abella, B., Rubio, L. and Rubio, P. (2012), "A non-destructive method for elliptical cracks identification in shafts based on wave propagation signals and genetic algorithms", *Smart Struct. Syst.*, **10**(1), 47-65.
- Oh, T., Popovics, J.S. and Sim, S.H. (2013), "Analysis of vibration for regions above rectangular delamination defects in solids", *J. Sound Vibr.*, **332**(7) 1766-1776.
- Ongpeng, J., Soberano, M., Oreta, A. and Hirose, S. (2017), "Artificial neural network model using ultrasonic test results to predict compressive stress in concrete", *Comput. Concrete*, **19**(1), 59-68.
- Park, C.B. (2011), "Imaging dispersion of MASW data-full vs. selective offset scheme", *J. Environ. Eng. Geophys.*, **16**(1), 13-23.
- Popovics, J.S., Song, W., Achenbach, J.D., Lee, J.H. and Andre, R.F. (1998), "One-sided stress wave velocity measurements in concrete", *J. Eng. Mech.*, **123**(12), 1346-1353.
- Prada, C. and Clorennec, D. (2009), "Influence of the anisotropy on zero-group velocity lamb modes", *J. Acoust. Soc. Am.*, **126**(2), 620-625.
- Sadeghi, J. and Rezvani, F.H. (2015), "Development of non-destructive method of detecting steel bars corrosion in bridge decks", *Struct. Eng. Mech.*, **46**(5), 615-627.
- Sheena, N.Y., Huangb, J.L. and Le, H.D. (2013), "Predicting strength development of RMSM using ultrasonic pulse velocity and artificial neural network", *Comput. Concrete*, **12**(6), 785-802.
- Song, H. and Popovics, J.S. (2017), "Characterization of steel-concrete interface bonding conditions using attenuation characteristics of guided waves", *Cement Concrete Compos.*, **83**, 111-124.
- Wright, P. (2010), "Assessment of London underground tube tunnels-investigation, monitoring and analysis", *Smart Struct. Syst.*, **6**(3), 239-262.
- Zhu, J. and Popovics, J.S. (2007), "Imaging concrete structures using air-coupled impact-echo", *J. Eng. Mech.*, **133**(6), 628-640.